frontiers in Earth Science

ORIGINAL RESEARCH
published: 22 August 2019
doi: 10.3389/feart.2019.00216

Terrain Induced Biases in Clear-Sky Shortwave Radiation Due to Digital Elevation Model Resolution for Glaciers in Complex Terrain

Matthew Olson[1], Summer Rupper[1] and David E. Shean[2]*

[1] Department of Geography, University of Utah, Salt Lake City, UT, United States, [2] Department of Civil and Environmental Engineering, University of Washington, Seattle, WA, United States

Advancements in remote sensing, along with greater access to high spatial and temporal resolution imagery, have improved our ability to model glacier surface energy and mass balance in remote regions of complex terrain, such as High-mountain Asia (HMA). In general, net shortwave (SW) radiation accounts for the majority of energy available on a glacier surface during the summer months, suggesting that SW modeling errors can critically impact surface energy balance estimates. In this study, we model the clear-sky SW irradiance for a group of glaciers in the Everest region of HMA using a high-resolution (8-m) digital elevation model (DEM) composite derived from commercial stereo satellite imagery. We then systematically downsample this DEM and considered the effect on incoming SW irradiance, with a sensitivity analysis for standard terrain attributes. The slope and aspect (combined) and topographic shading have the greatest impact on daily SW irradiance and also introduce a larger SW bias when DEM resolution is downsampled. Our results show that modeled incident SW is overestimated as resolution becomes coarser. For 10 selected glaciers in the Everest region, decreasing spatial resolution from 8 to 30 m results in a range of average daily biases between +20 and +60 Wm^{-2} (or ∼7 to 20%) at some high and low elevations, and an average bias of more than +100 Wm^{-2} (∼33%) as resolution is coarsened to 500 m. In order to determine the bearing these results have on surface melt, we explore the diurnal variability of this bias. Additionally, we compare our results with modeled incident SW using several global DEM products (ASTER, SRTM, and ALOS) to evaluate error introduced by lower resolution. Models using the 30-m products show an overall average daily SW bias of +24 Wm^{-2} (or ∼8%) across elevation with some elevations showing a bias up to +60 Wm^{-2} (∼20%) on multiple glaciers. Taken together, our results demonstrate the value of high-resolution data to correct biases in modeled SW radiation and constrain uncertainties for glacier energy balance modeling in regions of complex terrain.

Keywords: solar radiation, modeling, topography, energy balance, shortwave radiation, digital elevation model, glaciers

OPEN ACCESS

Edited by:
Markus Michael Frey, British Antarctic Survey (BAS), United Kingdom

Reviewed by:
Isabelle Gouttevin, Météo-France, France
Jakob Steiner, Utrecht University, Netherlands

****Correspondence:***
Matthew Olson
matthew.olson@geog.utah.edu;
olsonmeu@gmail.com

Specialty section:
This article was submitted to Cryospheric Sciences, a section of the journal Frontiers in Earth Science

Received: *01 May 2019*
Accepted: *07 August 2019*
Published: *22 August 2019*

Citation:
Olson M, Rupper S and Shean DE (2019) Terrain Induced Biases in Clear-Sky Shortwave Radiation Due to Digital Elevation Model Resolution for Glaciers in Complex Terrain. Front. Earth Sci. 7:216. doi: 10.3389/feart.2019.00216

INTRODUCTION

More than 1.4 billion people in Asia rely on freshwater that originates from remote High-mountain Asia (HMA) glaciers (Immerzeel et al., 2010). Often located in complex terrain, the ability to access and obtain *in situ* data in these landscapes can be difficult, if not impossible. As such, *in situ* data is sparse throughout the region. To address this problem, many studies rely on a combination of remote sensing and numerical modeling to determine the current state and future trends of HMA glaciers (Shea et al., 2015; Brun et al., 2017; Kraaijenbrink et al., 2017; Huss and Hock, 2018). Surface energy balance models provide a physically based approach to modeling glacier mass balance in HMA, and are a particularly important tool for assessing the causes of recent glacier change and projecting future glacier change (Kayastha et al., 1999; Azam et al., 2014; Litt et al., 2019).

Solar radiation, or shortwave (SW) radiation is a critical component of the surface energy balance (Cuffey and Paterson, 2010). SW radiation influences key energy balance terms and controls the overall variability in melt energy (Sicart et al., 2008). During (and prior to) the ablation season, when surface albedo is low, SW radiation is the dominant energy flux contributing to glacier melt (Arnold et al., 2006; Azam et al., 2014). However, incorporating terrain is essential in order to accurately model SW radiation — and surface energy balance — in remote alpine regions, where variable surface morphology and steep surrounding topography has the potential to drastically alter the SW component of the energy budget (Williams et al., 1972; Dozier, 1980; Duguay, 1993). The intensity of SW radiation at the ground surface is modified by terrain attributes such as slope, aspect, shading, elevation, and the portion of sky obstructed by surrounding terrain. Incorporating these attributes into solar radiation models improves accuracy of surface energy balance (Williams et al., 1972; Munro and Young, 1982; Kang et al., 2002). Although many surface energy balance models utilize meteorological station point data, energy fluxes must be distributed across the surface of a glacier in order to accurately quantify surface energy and mass balance. In many remote regions, where meteorological station data are not available, such as much of High Mountain Asia, energy fluxes are often derived from coarse resolution reanalysis products or climate models, and similarly must be distributed across the surface of a glacier. Solar radiation models incorporating terrain attributes provide the means by which to more accurately distribute solar radiation from either point source observations or coarse gridded climate products.

Terrain attributes are derived from digital elevation models (DEMs), and depend on the accuracy and spatial resolution of the DEM. Although high-resolution DEMs exist, coverage is limited, and many products are proprietary. Consequently, most glacier energy balance models have relied on coarse DEM resolution for surface topography, which can bias energy balance model results. For example, Olson and Rupper (2019) found that modeled direct solar radiation was increasingly overestimated when using a range of DEM resolutions from 30 to 1000 m, with the largest differences in direct shortwave radiation occurring when spatial resolution was coarsened from 30 to 60 and 90 m. Similarly, Hopkinson et al. (2010) found that continually decreasing DEM spatial resolution resulted in an increasing overestimation of modeled melt for a Canadian glacier. Although previous work shows terrain, and resolution of terrain, impacts results, this impact is likely not evenly distributed throughout the day. If the impact of terrain is most significant in the early mornings or late evenings, the influence on melt is likely minimal. High-temporal resolution modeling is required to capture the timing of terrain impact on SW and its potential importance in modeling glacier mass balance. While it may not be currently feasible to run a fully distributed energy balance model at high spatial and temporal resolution, using higher resolution to improve estimates or quantify uncertainty of net SW radiation across the surface of a glacier could improve modeled energy balance calculations, particularly during the ablation season.

While previous studies imply the importance of DEM spatial resolution on modeled surface energy balance and melt, they are often limited to expensive airborne imagery over few glaciers or utilize DEM resolutions of 30 m or lower. Additionally, results from these previous studies suggest the influence of topography on glacier surface energy balance will be amplified in regions of complex terrain, such as HMA, requiring higher resolution DEMs to adequately model SW radiation at glacier surfaces. The recent availability of sub-meter commercial stereo satellite image archives for scientific research and automated, open-source photogrammetry software (e.g., Shean et al., 2016; Noh and Howat, 2017) has led to a strong increase of publicly available high-resolution DEM products (e.g., Howat et al., 2007). As part of the NASA HiMAT project, Shean (2017) generated regional high-resolution (8-m) composite DEM products for HMA. This new product provides the opportunity to objectively evaluate the importance of terrain attributes and DEM resolution on remote glaciers in complex terrain, such as HMA.

In this study, we model the incident clear-sky SW radiation, including direct, diffuse, and reflected irradiance, on 10 glaciers of varying aspect and morphology in the Everest region (**Figure 1**). We evaluate the importance of each terrain attribute in modifying incident SW radiation for different times of the year on all 10 glaciers. Leveraging the new 8-m HiMAT DEM, we model SW radiation at a higher spatial resolution than was previously possible in this region. Furthermore, we assess the sensitivity of these results to different DEM spatial resolutions, and assess how these results vary throughout the day. The Everest region was selected because of the complex topography, presence of large glaciers with variable morphology, dense coverage of the 8-m HiMAT DEM, and large body of existing work on glaciers in the region. Thus the Everest region is a natural laboratory for assessing the importance of DEM resolution and terrain attributes on modeling SW radiation in HMA.

BACKGROUND

Incident SW radiation can be divided into three components: direct beam irradiance (I_b), scattered diffuse irradiance (I_d), and

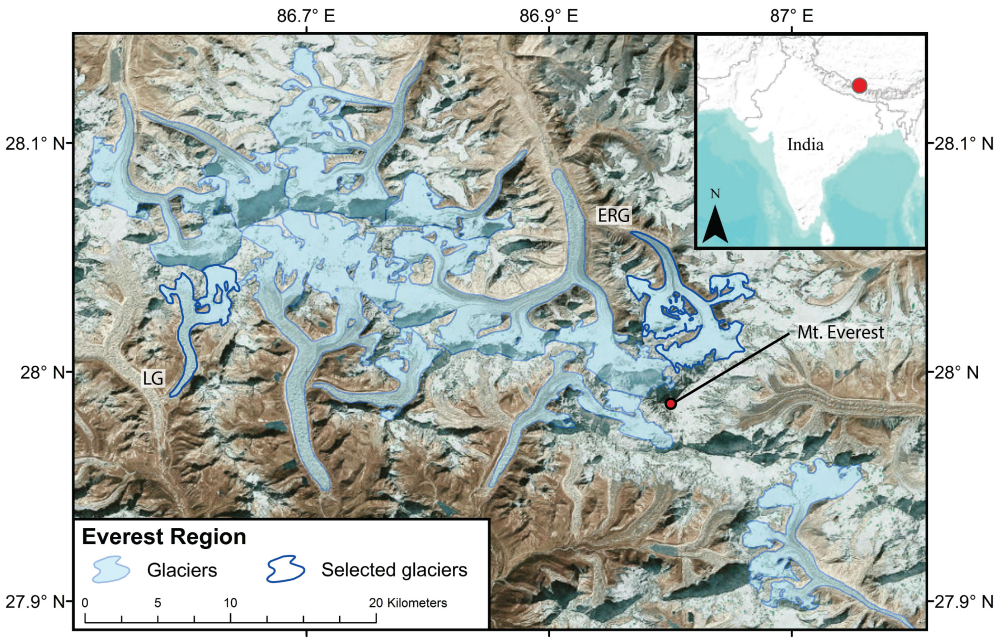

FIGURE 1 | Map of the Everest region in High-mountain Asia showing the 10 glaciers used in this study (light blue). The dark blue outlines indicate two selected glaciers, the East Rongbuk (ERG — RGI60-15.10055) and Lumsamba (LG — RGI60-15.03474), which we highlight throughout the paper. Glacier outlines from the Randolph Glacier Inventory v6.0 (RGI Consortium, 2017), basemap from Esri (2009).

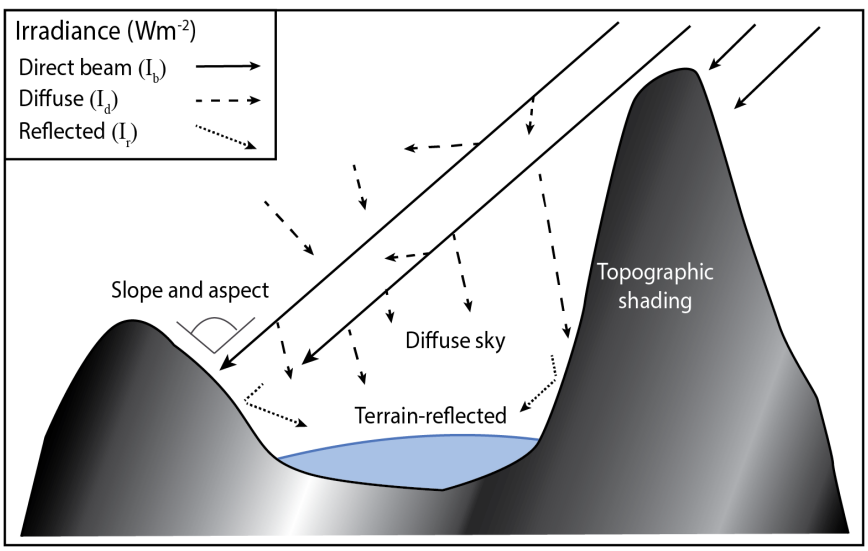

FIGURE 2 | Schematic showing how the three components of incident shortwave radiation — direct (I_b), diffuse (I_d), and reflected (I_r) irradiance — are altered by terrain. Topography alters shortwave radiation at the surface through the slope and aspect (generally combined), topographic shading, a decrease in the amount of diffuse sky radiation, and an increase in terrain-reflected radiation.

reflected irradiance (I_r) (Eq. 1) (Hock and Holmgren, 2005; Arnold et al., 2006).

$$SW_i = I_b + I_d + I_r \quad (1)$$

Figure 2 illustrates how these different irradiance components in Eq. (1) interact with the ground surface for an area of complex terrain.

Topography can either enhance or reduce solar radiation arriving at the surface of a glacier based on different terrain attributes; the slope and aspect, topographic shading, and the portion of sky visible at a given point known as the sky-view factor. Slope and aspect alter the direct beam irradiance by changing the solar zenith angle relative to a flat plane (e.g., in the northern hemisphere, a low-angle, south-facing slope

will receive more solar radiation, whereas a north-facing slope will receive less solar radiation throughout the day compared to a flat plane). The impact of slope and aspect on incident SW radiation is usually evaluated in combination with each other. Therefore, hereafter, we refer to this terrain attribute as *slope/aspect*. *Topographic shading* is a terrain attribute that refers to a decrease in direct beam irradiance either due to self-shading of a specific location, or from shadows cast by surrounding terrain. *Topographic shading* is mostly relevant in the morning and evening but can significantly alter daily irradiance on the surface of some glaciers (Arnold et al., 2006; Olson and Rupper, 2019). The sky-view factor is a terrain attribute that impacts both the amount of diffuse and reflected irradiances arriving at the surface. Because the sky-view factor inversely affects these two components of incident SW radiation, we keep their impact separate and refer to the terrain attributes related to the sky-view factor as *diffuse sky* and *terrain-reflected*. Diffuse irradiance is a complex function of multiple scattering and atmospheric composition; however, the sky-view factor decreases the amount of irradiance arriving at the surface due to the presence of surrounding terrain. *Terrain-reflected* irradiance is also a complicated term, as it consists of both direct and diffuse irradiance reflected from all surrounding visible terrain (Dozier, 1980; Duguay, 1993). *Terrain-reflected* irradiance only exists in the presence of surrounding topography, thus it is also considered a terrain attribute related to the sky-view factor.

Olson and Rupper (2019) found that the impact of *slope/aspect* and *topographic shading* on modeled clear-sky direct solar radiation is greatest in glacier valleys with an overall north or south valley aspect. Importantly, the majority of glaciers in HMA (40%) have a north or northeast valley aspect (Bajracharya and Shrestha, 2011). Olson and Rupper (2019) showed that these terrain attributes can reduce the average direct solar radiation during the summer melt season by upward of 80 Wm^{-2} relative to a flat, featureless plane. While these results illustrate the importance of these terrain attributes, the study only focused on direct beam irradiance and used a 30-m DEM to incorporate these terrain attributes in the solar radiation model. We build on this prior work by utilizing higher resolution DEMs and multiple DEM platforms, and by including diffuse and reflected irradiance in our model of incident SW radiation.

DATA AND METHODS

In this study, we run a clear-sky SW radiation model at a 15 min time-step, using the new 8-m HiMAT DEM on the spring equinox (March 21) and on the summer/winter solstices (June 21/December 21). The equinox roughly represents the average annual impact of topography on incident clear-sky SW for a glacier, while the two solstices represent the extreme ends of topography's influence for a glacier of specific morphology and latitude. We derive a change in irradiance, relative to a flat surface, due to each terrain attribute –*slope/aspect*, *topographic shading*, *diffuse sky*, *terrain-reflected* – for the East Rongbuk Glacier (RGI60 15.10055) and Lumsamba Glacier (RGI60 15.03474) on these three distinct days of the year. We highlight the results from these two glaciers to facilitate detailed discussion (**Figure 2**). We then assess the SW bias associated with downsampling the 8-m HiMAT DEM to lower spatial resolutions for all 10 glaciers in the Everest region, focusing on March 21. We also compare the sensitivity of terrain attributes at different spatial resolutions for the East Rongbuk Glacier and Lumsamba Glacier in order to determine which attributes have the largest contribution to the total bias in SW radiation. Although we show results for all 10 glaciers of varying aspect, we highlight results from the East Rongbuk Glacier and Lumsamba Glacier as they are north- and south-facing (respectively) and represent two distinct examples of how incident SW can be notably altered by local topography for glaciers in HMA. Finally, we compare the difference between modeling incident SW radiation with the 8-m HiMAT DEM to using other common 30-m DEM products.

Modeling Components of Incident SW Radiation

Direct beam irradiance (I_b) is typically the largest energy contribution to incident SW radiation, particularly under a clear-sky scenario. Fortunately, I_b is also the most straightforward component of SW radiation to model as it relies on solar geometry, day of the year, and atmospheric transmission. We use a broadband transfer equation to calculate direct irradiance through the atmosphere (Bird and Hulstrom, 1981; Mächler, 1983):

$$I_b = I_0 \cdot C \cdot \tau_R \cdot \tau_O \cdot \tau_G \cdot \tau_W \cdot \tau_A \quad (2)$$

where I_0 is extraterrestrial irradiance, incorporating both the solar constant and sun-earth distance, and C is a coefficient (0.9751). τ_R,τ_O,τ_G,τ_W, and τ_A represent the amount of transmittance through the atmosphere at a given moment due to Rayleigh scattering, ozone, mixed gases, atmospheric water vapor, and aerosols, respectively. The model used in this study is parameterized based on a local clear-sky scenario and uses a ground visibility estimate to calculate aerosol attenuation (Mächler, 1983). We follow methods from Corripio (2003) and Iqbal (1983) to calculate solar geometries, incidence angles, and topographic shading, which are further outlined in the following section.

Although modeling direct irradiance is generally simple, incorporating atmospheric scattering requires multiple model parameterizations and assumptions. Diffuse irradiance (I_d) is a complex function of multiple scattering and reflections based on atmospheric properties. In a clear-sky scenario the contribution from diffuse irradiance is generally small; however, its contribution can have a significant impact on daily incident SW irradiance, particularly when direct irradiance is intercepted by surrounding terrain. Bird and Hulstrom (1981) and Mächler (1983) describe methods for calculating atmospheric scattering in detail. Corripio (2014) has adapted these methods into an open-source library in R to compute solar radiation in complex terrain. We utilize the R insol library to compute both the direct and diffuse components of incident solar radiation.

Reflected irradiance (I_r) can contribute 17% of daily total SW radiation (Dozier, 1980). I_r relies on the amount of direct beam

and diffuse sky irradiance reflected from all visible surrounding terrain. Rather than attempting to accurately determine the albedo and scattering direction of radiation from all nearby terrain, solar radiation models often use a single value to represent the albedo of surrounding terrain and multiply the sky-view factor by the amount of direct and diffuse irradiance arriving on a flat plane (Eq. 3). Despite some oversimplifications in these methods, they have proven to be useful in modeling incident SW in complex terrain (Hock and Holmgren, 2005; Arnold et al., 2006).

Modeling Terrain Attributes

We model the daily mean change in irradiance due to each of the four different terrain attributes. To accomplish this, we build on Eq. (1) by incorporating terrain attributes into our model:

$$S_{\text{net}} = I_{\text{b}} S \cos\theta + V_{\text{f}} I_{\text{d}} + I_{\text{r}} \tag{3}$$
$$I_{\text{r}} = \alpha_{\text{t}} (1 - V_{\text{f}}) S_0$$

where S is topographic shading, θ is the incidence angle, V_{f} is a sky-view factor that indicates the portion of visible sky at a given location, a_{t} is the albedo of the surrounding terrain, and S_0 is the shortwave radiation incident on a flat plane for an entire basin. *Topographic shading* is calculated with a modified ray-tracing algorithm that uses the solar position at 15 min intervals to determine if a DEM grid cell is blocked by surrounding cells ($S = 0$), or is unobstructed ($S = 1$), at a certain zenith and azimuth angle (Corripio, 2003). The incident angle modifies the solar zenith angle for a surface with a specific slope and aspect. The incident angle is calculated as:

$$\cos\theta = \cos Z \cos S_{\text{slope}} + \sin Z \sin S_{\text{slope}} \cos(\phi - E) \tag{4}$$

where Z is the solar zenith angle, S_{slope} is slope, ϕ is azimuth, and E is exposure (i.e., the aspect with respect to a south-facing direction) (Iqbal, 1983). The incidence angle incorporates the impact associated with both the slope and aspect at the surface of a glacier at any moment during the day. The sky-view factor is calculated by determining the portion of visible sky in a 360° hemisphere at each point over a glacier surface (Dozier and Frew, 1990). An albedo of 0.45 is used to represent the reflectivity of surrounding terrain (Gratton et al., 1994).

In this study, we build on the methods of Olson and Rupper (2019) to model the change in irradiance due to each terrain attribute. The change in irradiance due to *slope/aspect* compares the difference between modeled incident SW radiation using the incidence angle and a model assuming a flat plane. The change in irradiance due to *topographic shading* is determined by the difference between a model that incorporates both cast shadows and self-shading and one that only utilizes slope and aspect at the surface to incorporate terrain effects. Changes in irradiance related to both *diffuse sky* and *terrain-reflected* irradiances are determined by the difference between a model that incorporates the sky-view factor and one that assumes the sky-view factor is equal to 1. Additionally, we model the *combined* effect of all terrain attributes on daily incident SW radiation. The change in irradiance for the *combined* effect is determined by the difference between a model incorporating all terrain attributes and a model calculating incident SW radiation on a flat plane. The modeled daily mean change in irradiance across glacier elevation is fit with a cubic smoothing spline. This allows us to compare terrain attributes to one another, and observe the variability across low (ablation zone) and high (accumulation zone) elevations.

DEM Downscaling and Comparison

Quantifying the impact of terrain attributes on modeled SW radiation relies on the accuracy and resolution of the DEM used. The 8-m HiMAT DEM was generated by adapting the open-source NASA Ames Stereo Pipeline and orthoimages from DigitalGlobe WorldView-1, WorldView-2, WorldView-3 and GeoEye-1 stereo imagery over HMA (Shean, 2017). Blended mosaics are produced from optical images obtained between 2008 and 2017, with the majority of coverage from 2013 to 2016. Approximately 5700 DEMs were generated for glacierized portions of HMA, and a tiled composite of DEM products are posted at 8-m. Shean et al. (2016) provide detailed information of the DEM processing pipeline and validate the accuracy of DEMs in the polar regions, while Shean (2017) includes a description of processing and error sources for the 8-m HiMAT DEM.

To test the effects of different DEM resolutions, we downsample the 8-m HiMAT DEM to resolutions commonly used by the modeling community – 30, 90, 250, and 500 m. To avoid aliasing, we use a low-pass Gaussian filter with a 5 × 5 pixel kernel, followed by bilinear interpolation of the filtered DEM. We calculate the incident SW (Combined effect) bias at each downsampled DEM resolution, relative to the 8-m HIMAT DEM, for 10 glaciers in the Everest region. We also compare the inter-glacier variability in SW bias for the downsampled 30- and 90-m resolutions. Finally, we calculate the SW bias for each of the four terrain attributes to determine which terrain attributes contribute most to the SW bias.

Currently, several publicly available 30-m resolution DEM products are available with global or near-global coverage. These include products from the Advanced Spaceborne Thermal Emission and Reflection Radiometer (ASTER), the Shuttle Radar Topography Mission (SRTM), and more recently the Advanced Land Observing Satellite (ALOS). Glacier modeling studies often use one of these three DEMs (Lee et al., 2012; Chen et al., 2013; Huintjes et al., 2015; Han et al., 2016). We evaluate bias introduced by using these lower-resolution products to simulate terrain in our topographic SW radiation model. In addition to determining the modeled SW bias from Combined terrain attributes, we compare these DEMs to the downsampled 30-m HiMAT DEM to further test the utility of the 8-m HiMAT DEM.

RESULTS

The sensitivity of daily incident SW radiation to terrain attributes varies significantly, both in magnitude and sign, between the equinox and solstices. However, the combined influence of terrain leads to a decrease in incident SW radiation when averaged annually for glaciers in the Everest region. Coarser DEM resolution causes an overestimation in incident SW radiation,

and a similar daily SW bias is observed when using common 30-m resolution DEM products. Each of these findings is presented in detail below.

Spatial and Temporal Variability in Modeled Incident SW

Figure 3 shows the daily averaged change in irradiance along elevation due to each terrain attribute and the *combined* effect for East Rongbuk Glacier and Lumsamba Glacier. During March, which represents the average annual impact of terrain on incident SW radiation, the East Rongbuk Glacier has a significant decrease in irradiance from combined terrain attributes, largely due to its north-facing orientation (**Figure 3A**). Meanwhile, the different terrain attributes offset the change in SW radiation across the south-facing Lumsamba Glacier (**Figure 3B**), primarily driven by the opposing influences of *slope/aspect* and *topographic shading*. With higher solar zenith angles in June, the change in irradiance due to *slope/aspect* and *topographic shading* for these relatively low latitude glaciers (∼26° N) decreases for the East Rongbuk Glacier and increases for the Lumsamba Glacier (**Figure 3D**). The largest contrast in the combined change in irradiance for these two glaciers is during the winter months (December). During this time of the year, low solar zenith angles cast shadows over the north-facing East Rongbuk Glacier for a significant part of the day, causing a large decrease in SW radiation (**Figure 3E**). The lowest values (around $-400\ \mathrm{Wm^{-2}}$) represent a nearly 100% decrease in irradiance at highest elevations due to the combined impact of terrain attributes during this time of year. Alternatively, the *slope/aspect* greatly increases irradiance on the south-facing Lumsamba Glacier during the winter solstice (**Figure 3F**). These results show that the impact of terrain on SW radiation is distinct during different times of the year and varies between glaciers. Much of the difference between glaciers is driven by their overall aspect.

More generally, terrain attributes have a greater impact on SW radiation at mid- to upper-elevations on both East Rongbuk Glacier and Lumsamba Glacier; however, changes in irradiance at lower elevations are also significant. *slope/aspect* and *topographic shading* are the most variable and influential terrain attributes affecting daily SW radiation throughout the year. By comparison, the influence of *diffuse-sky* and *terrain-reflected* irradiance is similar for both glaciers and varies much less in comparison to the other terrain attributes, and from season to season. Though seasonal variations are significant, the average annual change in irradiance due to *combined* terrain attributes is negative for both glaciers.

SW Bias Due to DEM Resolution

While terrain attributes can significantly change irradiance values on the surface of a glacier throughout the year, these attributes are

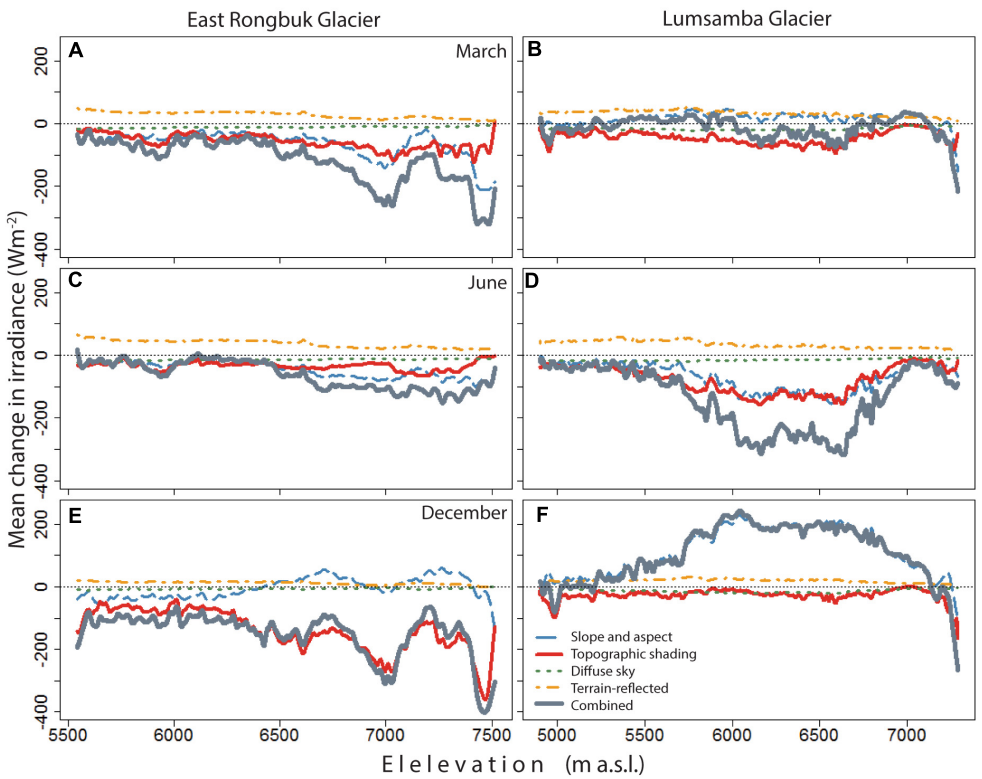

FIGURE 3 | Daily mean change in irradiance vs. elevation due to different terrain attributes (and their combined effect) for East Rongbuk Glacier (left panels) and Lumsamba Glacier (right panels). The model is run on the spring equinox—March 21 **(A,B)**, summer solstice—June 21 **(C,D)**, and winter solstice—December 21 **(E,F)**.

dependent on DEM resolution (**Figure 4**). As the HiMAT DEM resolution is progressively coarsened from 8 m to 30, 90, 250, and 500 m, topographic variability and detail decreases, which decreases the magnitude and variability in terrain features. As a result, all 10 glaciers in the Everest region exhibit an increasingly positive bias (or anomaly) in SW radiation as the 8-m HiMAT DEM resolution is downsampled. All biases are calculated as the difference in modeled incident SW for the downsampled DEM relative to the 8-m HiMAT DEM. The details of this positive bias can be seen in **Figure 4A**, which shows the SW anomaly averaged across all 10 glaciers for each resolution on the spring equinox. The largest bias appears to be at higher relative elevations and becomes greater as the DEM is downsampled to the coarsest resolutions.

Figures 4B,C show the SW bias for each glacier as resolution is coarsened to 30 and 90 m, and illustrate the substantial inter-glacier variability in the SW bias for these resolutions. Overall, downsampling DEM resolution from 8 to 30 m results in average daily positive biases that range between 20 and 60 Wm^{-2} (or ∼7 to 20%) at certain elevations (**Figure 4B**). At 90 m (**Figure 4C**), we see an even greater increase in the SW bias for all glaciers as compared to 30 m; however, higher elevations and certain glaciers are more impacted as the DEM is downsampled to these progressively lower spatial resolutions. At 500-m resolution (not shown here), many of the 10 glaciers have a combined bias of more than +100 Wm^{-2} (∼33%) at multiple elevations, with some glaciers having an average SW bias upward of +250 Wm^{-2} (∼83%). While the bias tends to be overwhelmingly positive as DEM resolution is coarsened, upper elevations on some glaciers do show a negative SW bias.

In order to determine which terrain attributes are the largest contributors to the overall combined SW bias, we compare the modeled SW bias for each terrain attribute, and at all downsampled DEM resolutions. **Figure 5** shows the SW anomalies, relative to the 8-m DEM, for each terrain attribute for East Rongbuk Glacier and Lumsamba Glacier during the spring equinox (March 21). Anomalies for the East Rongbuk Glacier (**Figure 5a**) show that *slope/aspect* contributes a positive SW bias at low elevations and a negative bias at high elevations as terrain is progressively smoothed. *Topographic shading* has the largest influence on the SW bias as DEM resolution degrades. The *diffuse sky* and *terrain-reflected* biases have contrasting effects, and contribute much less to SW biases. Specifically for the *combined* effects, as spatial resolution decreases from 8 to 30 m, the average daily SW bias for East Rongbuk Glacier is upward of +50 Wm^{-2} (∼17%) at certain elevations. Further lowering the resolution to 500 m results in a bias upward of +85 Wm^{-2} (∼28%).

The results for Lumsamba Glacier (**Figure 5b**) provide an interesting comparison to East Rongbuk Glacier. SW anomalies across varying DEM resolutions for Lumsamba Glacier (**Figure 5b**) show similar patterns to East Rongbuk Glacier; however, the overall bias is larger for the Lumsamba Glacier due in part to a more positive SW bias from the *slope/aspect* across all elevations and an increased influence from *topographic shading* at certain elevations. It should also be noted that the *terrain-reflected* bias is more negative for this south-facing glacier because it has more visible surrounding terrain (i.e., smaller view factor). Similar to East Rongbuk Glacier, the *combined* daily shortwave bias is ∼15–30% when the DEM resolution is downsampled from 30- to 500-m resolution.

Figure 5c shows the spatial variability in the *combined* change in irradiance due to all terrain attributes for East Rongbuk Glacier at each of the downsampled resolutions. The results further illustrate that incident SW is overestimated, but spatially variable, as resolution is downsampled.

Diurnal Differences in SW Irradiance

The above results highlight the impact of terrain on daily averaged clear-sky SW irradiance, and illustrate how modeled SW irradiance is overestimated at coarser DEM resolutions. However, the magnitude of change on modeled SW, due to both terrain and DEM resolution, varies considerably throughout the day. Thus, depending on the time of day, changes in energy at the surface of a glacier may affect melt, refreezing, or merely alter

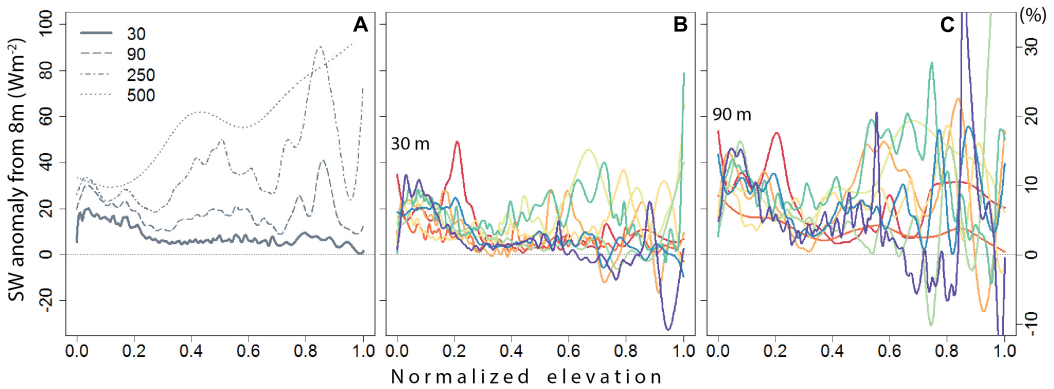

FIGURE 4 | Shortwave anomalies (due to the combined effect of terrain attributes) averaged across all 10 glaciers in the region as resolution is coarsened to 30-, 90-, 250-, and 500-m resolutions **(A)**. Panels **(B,C)** show the SW anomaly values at 30- and 90-m resolutions (respectively) for each glacier in the Everest region. Note that the SW anomalies vary drastically from glacier to glacier. The change in irradiance from terrain attributes accounts for variability in irradiance across elevation, thus we show absolute anomalies (left y-axis) in conjunction with percent changes (right y-axis) relative to the mean irradiance over the glaciers.

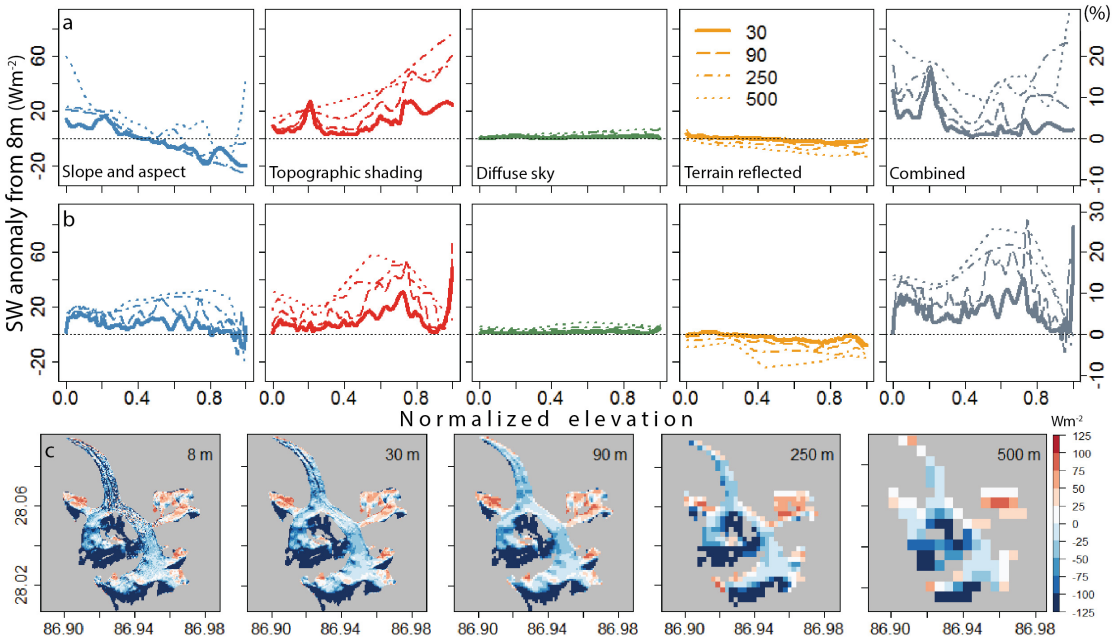

FIGURE 5 | Shortwave anomaly for 30-, 90-, 250-, and 500-m resolutions, relative to the 8-m HIMAT DEM, for the East Rongbuk Glacier (**a**, top panels) and the Lumsamba Glacier (**b**, middle panels) on March 21. The contribution of each terrain attribute to the modeled SW bias is shown at each downsampled DEM resolution, along with the combined bias from all terrain attributes. Overall, incident SW radiation is overestimated when resolution is coarsened. For both glaciers, the combined bias is most impacted by changes in modeled topographic shading and slope/aspect, while the change from diffuse sky and terrain-reflected are smaller in magnitude and vary less at different spatial resolutions. This holds true for all 10 glaciers in this study. Panel **(c)** shows the combined change in irradiance due to all terrain attributes on this day at each downsampled resolution for East Rongbuk Glacier. The SW anomaly is the difference between the change in irradiance determined at each coarse DEM resolution relative to the change in irradiance calculated with the 8-m HIMAT DEM.

the temperature at the surface (i.e., the cold content). While changes in modeled SW during the morning/evening may alter the timing and magnitude of melt later in the day, accurately capturing changes in incident SW during mid-day are more crucial for estimating energy balance and total surface melt. Here we assess how terrain and DEM resolution alter the diurnal cycle in incident SW irradiance.

Figure 6a shows the change in incident clear-sky SW irradiance due to *slope/aspect* across elevation and at each 15 min time-step on March 21, 2019 for East Rongbuk Glacier. **Figure 6b** shows the SW bias introduced from the *slope/aspect* when modeling SW irradiance at 30-m resolution, as opposed to 8-m resolution. **Figure 6c** shows the SW bias when modeling at 90-m resolution. Incident SW on this north-facing glacier is enhanced in the morning/evening and reduced during mid-day along most elevations (**Figure 6a**). However, as DEM resolution is coarsened (**Figures 6b,c**), there is a decrease in SW during the morning/evening and an increase during mid-day as the terrain is smoothed at lower elevations. At upper elevations the bias is greater and more variable, though generally shows an overall negative bias, which can be seen in the daily averaged values (**Figure 5a**). The large increase in SW at high elevations during the morning (**Figure 6a**) is due to an east-facing upper bowl of the glacier. The additional panel rows on **Figure 6** show the same results but for the change in SW due to *topographic shading* and due to *combined* terrain attributes, followed by the SW anomaly at 30 and 90 m for each. We focus on the two largest terrain attributes, *slope/aspect* and *topographic shading,* as they largely control the overall *combined* change in irradiance. Although *topographic shading* has the greatest impact during mid-morning, it influences most glacier elevations throughout the day. Similarly, the bias at 30 and 90 m shows an overestimation of incident SW throughout the day along most elevations. The *combined* results show an overall estimation of SW irradiance throughout the day as resolution is coarsened. While topography has a variable effect throughout the day and along elevation, the greatest positive SW bias generally occurs during warmer hours of the day when modeling SW irradiance at coarser resolution. Similar to the results for daily-average SW, the role of terrain and DEM resolution varies between glaciers and differing times of the year. However, these results illustrate that terrain attributes and DEM resolution can impact modeled SW irradiance during the peak energy flux of the day, and therefore can introduce bias in modeled melt.

SW Bias Due to DEM Platform

With the availability of many 30-m DEMs for remote regions of complex terrain, such as HMA, we also evaluate the SW bias (anomaly) associated when modeling SW radiation using different DEM products. **Figure 7** compares the combined SW bias of four different 30-m resolution DEMs,

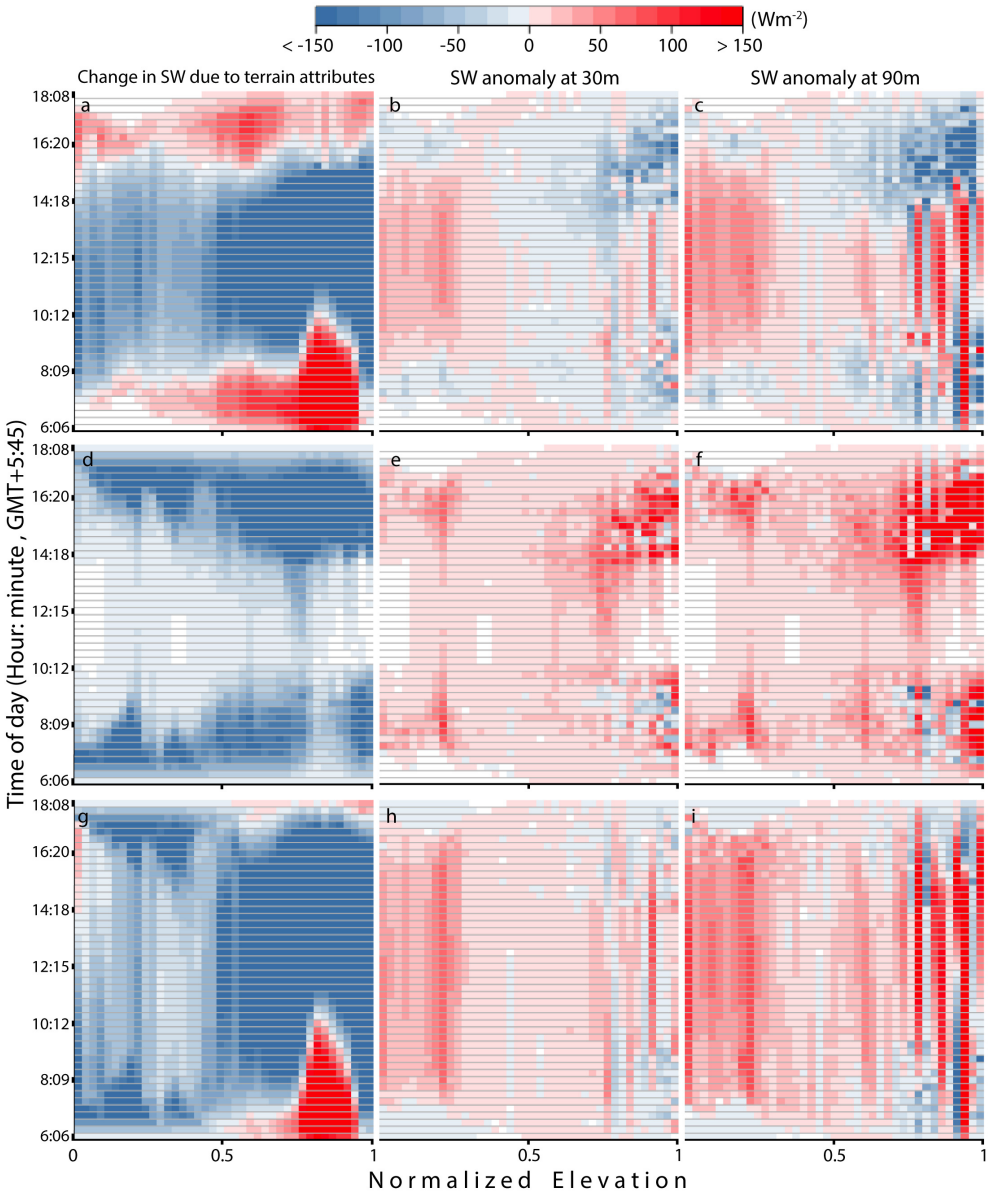

FIGURE 6 | Change in incident SW irradiance due to slope/aspect **(a)** for East Rongbuk Glacier (calculated with the 8-m HiMAT DEM). Sunrise (Sunset) occurs at 6:06 am (8:09 pm) local time on March 21, 2019 at this glacier. The y-axis shows the time stamp at 15 min intervals, starting at sunrise and ending at sunset. The anomaly (or bias) introduced by the change in slope/aspect when modeling SW irradiance at 30-m DEM resolution, as opposed to 8-m resolution **(b)**, and the bias added to slope/aspect from modeling at 90-m resolution **(c)**. The subsequent panel rows show the same change in irradiance and SW biases for topographic shading **(d–f)** and combined terrain attributes **(g–i)**. Values are aggregated into 50-m elevation bins and color scale changes in increments of ± 15 Wm^{-2}.

relative to the 8-m HiMAT DEM. For convenience and consistency, we show the results for East Rongbuk Glacier and Lumsamba Glacier. SW bias values for East Rongbuk Glacier (**Figure 7A**) show a mostly consistent positive bias for most 30-m DEMs. SW biases from the SRTM and ALOS DEMs show very similar values, while the biases from the ASTER GDEM differ drastically at some elevations. The bias from the downsampled 30-m HiMAT DEM is most similar to SRTM and ALOS values, though smaller in magnitude on average.

The SW bias values of the different DEM products for Lumsamba Glacier show greater consistency and an overall positive SW bias (**Figure 7B**). Again, bias values from SRTM and ALOS are most similar, with ASTER having more variation. When comparing values for all 10 glaciers (not shown here), ASTER has more overall variation in SW bias as compared with SRTM and ALOS, but rarely shows significant deviations from these other products. Additionally, the fact that the 30-m downsampled HiMAT DEM compares reasonably well to other 30-m DEMs suggests that our downsampling methods are likely

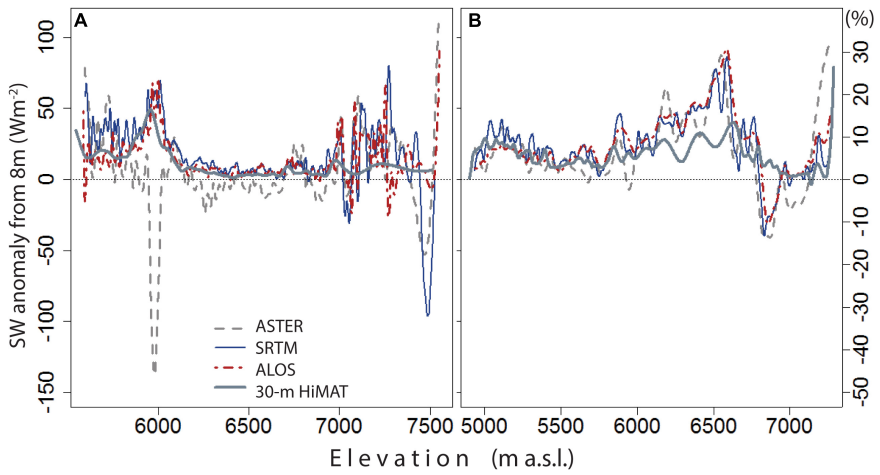

FIGURE 7 | Modeled shortwave bias, relative to the 8-m HiMAT DEM, for each 30-m DEM product (i.e., ASTER GDEM, SRTM, ALOS, and coarsened 30-m HiMAT DEM) on the East Rongbuk Glacier **(A)** and the Lumsamba Glacier **(B)** on March 21. An average daily overestimation of ∼50–60 W m^{-2} (∼20%) of incident SW radiation is common across many elevations when resolution is coarsened to 30-m, with some glaciers exhibiting average biases upward of 90 W m^{-2} (∼30%). Although the SW bias is mostly similar between DEM products, bias values from ASTER can vary drastically at some glacier elevations **(A)**, however, ASTER is often more consistent across all 10 glaciers, similar to **B**.

reasonable. Overall, modeling at a 30-m spatial resolution can introduce a bias upward of +60 Wm^{-2} (∼20%) over the course of a single day at some glacier elevations, and this result is generally true for all DEM products tested here.

DISCUSSION

The results of this study strongly indicate that modeling the variability of incident SW radiation in complex terrain requires high spatial resolution in order to resolve the influence of terrain attributes throughout the day. However, the overall importance of terrain and the accuracy of modeling terrain interactions with incident SW radiation will also depend on other variables not directly addressed in this study, such as: local topographic and meteorological conditions (esp. cloudiness conditions), assumptions/parameterizations in the SW model, and on the accuracy of the DEMs.

As sun angles vary throughout the day at a given location, the influence of specific terrain attributes changes in magnitude and sometimes sign. *Slope/aspect* and *topographic shading* are the most variable and impactful terrain attributes that modify daily SW radiation on glaciers in HMA (**Figure 3**). These two terrain attributes vary drastically based on their relationship with solar angles throughout the day, seasonally, and between glacier valleys. While incorporating *slope/aspect* into SW radiation models is fairly simple, correctly incorporating the effect of shadows cast from surrounding topography requires additional complexity; consequently, many energy balance models incorrectly incorporate shading or do not include it at all (Olson and Rupper, 2019). By comparison, *diffuse sky* irradiance is more temporally consistent than *slope/aspect* or *topographic shading*, as this terrain attribute mostly relies on static sky-view factors across the glacier surface. *Terrain-reflected* irradiances also depend on temporally static sky-view factors. However, the magnitude of *terrain-reflected* irradiance is dependent on the albedo of the surrounding terrain and other model simplifications, which can vary more significantly over space and time. Our assumption of a constant albedo of 0.45 is a significant oversimplification in the model. While this represents a reasonable value for the albedo of glacier ice (Gratton et al., 1994), it certainly underestimates the albedo of surrounding terrain in some locations and overestimates in others. However, using an albedo of 0.30 and 0.60 only modifies the daily mean change in *terrain-reflected* irradiance by ±3.3% with a standard deviation of 1.4%. Thus the chosen albedo value is unlikely to significantly impact the key result, that *terrain-reflected* irradiances generally have a significantly smaller impact on clear sky SW irradiance as compared to *slope/aspect* and *topographic shading*.

While topography has a large effect on incident SW radiation, the magnitude of this effect is dependent on the variability in atmospheric conditions (which is not captured in this study). The results in this study are based on a clear-sky solar radiation model; however, incident SW is also impacted by atmospheric properties and cloud cover, both of which can significantly diminish the impact of terrain on SW radiation. For example, cloudy conditions cause a lower intensity of direct beam irradiance to be obstructed by surrounding terrain, lessening the importance of *topographic shading* on a glacier's surface. Despite some model simplifications and assumptions, the big picture results are likely robust. Specifically, terrain tends to reduce daily SW radiation at a glacier surface; therefore, excluding terrain attributes will lead to an overestimation in modeled energy and melt at the glacier surface. Additionally, this study has application for fields beyond the glacier community, as solar radiation is also an essential variable in snow, ecosystem, and forestry modeling (Comola et al., 2015; Baba et al., 2019; Wu et al., 2019).

An overestimation of incident SW can also result from modeling with coarser DEM resolutions, and this overestimation can occur throughout the day. Coarsening DEM resolution, on average, gives rise to a progressively larger positive bias in incident SW (**Figure 4A**). However, a significant portion of error is introduced on many glaciers even when downsampling from 8 to 30 or 90 m (**Figures 4B,C**). For example, the combined SW bias at 30 m is quite large for some glaciers, suggesting that even a decrease in accuracy of ∼22 m can seriously bias modeling results. These SW biases are present at both lower and upper elevations, and vary between glacier basins. Overestimating SW radiation at lower elevations, where temperatures are higher and melt is more likely to occur, can significantly change surface energy balance modeling results and lead to overestimating melt at the glacier surface. When modeling with very coarse DEM resolutions (250 or 500 m), changes in incident SW radiation due to terrain attributes are inadequately represented and can introduce significant errors in SW radiation, and these errors propagate into the modeled glacier mass balance and melt. The modeled SW bias due to decreasing DEM resolution is primarily due to changes in modeled *slope/aspect* and *topographic shading*, once again highlighting the importance of these terrain attributes for surface energy balance modeling. Additionally, we see that there is a modeled bias in incident SW throughout the warmer hours of the day (**Figure 6**) as DEM resolution is coarsened, illustrating the importance of resolution for modeling melt.

When comparing the accuracy of modeled SW radiation between DEM products, we see a mostly consistent positive SW bias for all products relative to the higher resolution DEM. The bias from the ASTER GDEM shows the most variation for some glacier elevations, particularly at lower elevations, but is overall similar to other products. Nascetti et al., 2017 found that the accuracy of the SRTM DEM is generally more accurate over flat terrain, whereas the accuracy of the ASTER DEM performed better at steeper slope angles, which could explain the variability we see on East Rongbuk Glacier. However, for all 10 glaciers we generally see a consistent SW bias between all DEM products, suggesting a similar accuracy in modeled SW for most glaciers in this region. Importantly, the modeled SW bias from the downsampled 30-m HiMAT DEM is consistent, though smaller in magnitude, with other DEM products (**Figure 7**). These consistencies validate our downsampling analysis, and the lower magnitude of SW bias in the 30-m HiMAT DEM is likely due to it being directly downsampled from the 8-m product. In general, these results show that modeled SW radiation will depend primarily on DEM resolution, and secondarily on the DEM product. However, modeled SW radiation will also be impacted by the accuracy of the DEMs, which is not directly evaluated in this study.

CONCLUSION

In this study, we model direct, diffuse, and reflected SW irradiance on 10 glaciers in the Everest region of HMA. We compare the relative importance of slope and aspect, shading by topography, and the sky-view factor on the incident SW radiation, and assess the sensitivity of these results to DEM resolution and platform. Overall, *slope/aspect* and *topographic shading* have the greatest impact on daily incident SW, while the sky-view factor (due to both *diffuse sky* and *terrain-reflected* irradiances) contributes significantly less. The degree to which these terrain attributes alter the modeled SW irradiances also depends on the DEM resolution used. Modeling SW at 30-m spatial resolution, as compared to the new 8-m HiMAT DEM, can introduce a positive SW bias between 20 and 60 Wm^{-2} (∼7–20%) along some glacier elevations, which increases to upward of 100 Wm^{-2} (∼33%) as resolution coarsens to 500 m. This bias is primarily driven by the error in estimating *topographic shading* and *slope/aspect* at lower DEM resolutions, and less by changes in the sky-view factor. For all glaciers in this study, we demonstrate a systematic overestimation in daily modeled SW radiation with decreasing DEM spatial resolution. Additionally, we see that common 30-m DEM products can introduce a significant bias in incident SW (+60 to + 90 Wm^{-2} or ∼20 to 30%) at certain elevations compared to the 8-m HiMAT DEM. These results can be utilized as a bias correction for modeled incident SW in the region, or used to better constrain uncertainty in model results. We also see that the positive bias introduced when modeling incident SW at lower DEM resolutions occurs throughout the warmer hours of the day, which would lead to a higher bias in modeled melt. In summary, correctly modeling the impact of terrain and utilizing high spatial resolution, such as the 8-m HiMAT DEM, are essential to accurately quantifying incident SW energy and melt on glaciers in complex terrain.

DATA AVAILABILITY

Shean (2017) has made the 8-m HiMAT DEMs publicly available through the NASA National Snow and Ice Data Center Distributed Active Archive Center (https://doi.org/10.5067/KXOVQ9L172S2). Model code is available at: http://doi.org/10.5281/zenodo.2654938 (Olson, 2019).

AUTHOR CONTRIBUTIONS

MO and SR designed the study and wrote the manuscript. MO developed the model, performed the analysis, and generated the figures. DS generated the 8-m HiMAT DEM and provided feedback and comments for text and figures.

FUNDING

This research was funded as part of the NASA HiMAT (NASA HMA NNX16AQ61G, awarded to SR).

ACKNOWLEDGMENTS

We would like to acknowledge the valuable feedback and support from the NASA HiMAT.

REFERENCES

Arnold, N. S., Rees, W. G., Hodson, A. J., and Kohler, J. (2006). Topographic controls on the surface energy balance of a high Arctic valley glacier. *J. Geophys. Res.* 111:F02011. doi: 10.1029/2005jf000426

Azam, M. F., Wagnon, P., Vincent, C., Ramanathan, A., Favier, V., Mandal, A., et al. (2014). Processes governing the mass balance of Chhota Shigri Glacier (western Himalaya, India) assessed by point-scale surface energy balance measurements. *Cryosphere* 8, 2195–2217. doi: 10.5194/tc-8-2195-2014

Baba, M. W., Gascoin, S., Kinnard, C., Marchane, A., and Hanich, L. (2019). Effect of digital elevation model resolution on the simulation of the snow cover evolution in the High Atlas. *Water Resour. Res.* 55, 1–19. doi: 10.1029/2018WR023789

Bajracharya, S. R., and Shrestha, B. (eds) (2011). *The Status of Glaciers in the Hindu Kush-Himalayan Region*. Kathmandu: ICIMOD.

Bird, R. E., and Hulstrom, R. L. (1981). *Simplified Clear Sky Model for Direct and Diffuse Insolation on Horizontal Surfaces. Technical Report SERI/TR-642-761*, Golden, CO: Solar Research Institute, 1–38. doi: 10.2172/6510849

Brun, F., Berthier, E., Wagnon, P., Kääb, A., and Treichler, D. (2017). A spatially resolved estimate of high mountain asia glacier mass balances from 2000 to 2016. *Nat. Geosci.* 10, 668–673. doi: 10.1038/NGEO2999

Chen, X., Su, Z., Ma, Y., Yang, K., and Wang, B. (2013). Estimation of surface energy fluxes under complex terrain of Mt. Qomolangma over the Tibetan Plateau. *Hydrol. Earth Syst. Sci.* 17, 1607–1618. doi: 10.5194/hess-17-1607-2013

Comola, F., Schaefli, B., Da Ronco, P., Botter, G., Bavay, M., Rinaldo, A., et al. (2015). Scale-dependent effects of solar radiation patterns on the snow-dominated hydrologic response. *Geophys. Res. Lett.* 42, 3895–3902. doi: 10.1002/2015gl064075

Corripio, J. G. (2003). Vectorial algebra algorithms for calculating terrain parameters from DEMs and solar radiation modelling in mountainous terrain. *Int. J. Geogr. Inform. Sci.* 17, 1–23. doi: 10.1080/713811744

Corripio, J. G. (2014). *Insol: Solar Radiation. R Package Version 1.1.1*. Available at: https://CRAN.R-project.org/package=insol (accessed August 21, 2018).

Cuffey, K. M., and Paterson, W. S. B. (2010). *The Physics of Glaciers*. Cambridge, MA: Academic Press.

Dozier, J. (1980). A clear-sky spectral solar radiation model for snow-covered mountainous terrain. *Water Resour. Res.* 16, 709–718. doi: 10.1029/wr016i004p00709

Dozier, J., and Frew, J. (1990). Rapid calculation of terrain parameters for radiation modeling from digital elevation data. *IEEE Trans. Geosci. Remote Sens.* 28, 963–969. doi: 10.1109/36.58986

Duguay, C. R. (1993). Radiation modeling in mountainous terrain review and status. *Mount. Res. Dev.* 13, 339–357. doi: 10.2307/3673761

Esri (2009). *World Imagery*. Available at: http://www.arcgis.com/home/item.html?id=10df2279f9684e4a9f6a7f08febac2a9 (accessed August, 21 2018).

Gratton, D. J., Howarth, P. J., and Marceau, D. J. (1994). An investigation of terrain irradiance in a mountain-glacier basin. *J. Glaciol.* 40, 519–526. doi: 10.3189/s0022143000012405

Han, C., Ma, Y., Chen, X., and Su, Z. (2016). Estimates of land surface heat fluxes of the Mt. Everest region over the Tibetan Plateau utilizing ASTER data. *Atmos. Res.* 168, 180–190. doi: 10.1016/j.atmosres.2015.09.012

Hock, R., and Holmgren, B. (2005). A distributed surface energy-balance model for complex topography and its application to Storglaciären, Sweden. *J. Glaciol.* 51, 25–36. doi: 10.3189/172756505781829566

Hopkinson, C., Chasmer, L., Munro, S., and Demuth, M. N. (2010). The influence of DEM resolution on simulated solar radiation-induced glacier melt. *Hydrol. Process.* 24, 775–788. doi: 10.1002/hyp.7531

Howat, I. M., Joughin, I., and Scambos, T. A. (2007). Rapid changes in ice discharge from greenland outlet glaciers. *Science* 315, 1559–1561. doi: 10.1126/science.1138478

Huintjes, E., Sauter, T., Schröter, B., Maussion, F., Yang, W., Kropáček, J., et al. (2015). Evaluation of a coupled snow and energy balance model for Zhadang glacier, Tibetan Plateau, using glaciological measurements and time-lapse photography. *Arct. Antarct. Alp. Res.* 47, 573–590. doi: 10.1657/aaar0014-073

Huss, M., and Hock, R. (2018). Global-scale hydrological response to future glacier mass loss. *Nat. Clim. Change* 8, 135–140. doi: 10.1038/s41558-017-0049-x

Immerzeel, W. W., Beek, L. P. H. V., and Bierkens, M. F. P. (2010). Climate change will affect the asian water towers. *Science* 328, 1382–1385. doi: 10.1126/science.1183188

Iqbal, M. (1983). *An Introduction to Solar Radiation*. Toronto, ON: Academic Press.

Kang, S., Kim, S., and Lee, D. (2002). Spatial and temporal patterns of solar radiation based on topography and air temperature. *Can. J. For. Res.* 32, 487–497. doi: 10.1139/x01-221

Kayastha, R. B., Ohata, T., and Ageta, Y. (1999). Application of a mass-balance model to a Himalayan glacier. *J. Glaciol.* 45, 559–567. doi: 10.3189/s002214300000143x

Kraaijenbrink, P. D. A., Bierkens, M. F. P., Lutz, A. F., and Immerzeel, W. W. (2017). Impact of a global temperature rise of 1.5 degrees Celsius on Asia's glaciers. *Nature* 549, 257–260. doi: 10.1038/nature23878

Lee, W.-L., Liou, K. N., and Wang, C.-C. (2012). Impact of 3-D topography on surface radiation budget over the Tibetan Plateau. *Theor. Appl. Climatol.* 113, 95–103. doi: 10.1007/s00704-012-0767-y

Litt, M., Shea, J., Wagnon, P., Steiner, J., Koch, I., Stigter, E., et al. (2019). Glacier ablation and temperature indexed melt models in the Nepalese Himalaya. *Sci. Rep.* 9:5264. doi: 10.1038/s41598-019-41657-5

Mächler, M. A. (1983). *Parameterization of Solar Irradiation Under Clear Skies*, Vancouver, CA: Doctoral dissertation, University of British Columbia, 1–93. doi: 10.14288/1.0080802

Munro, D. S., and Young, G. J. (1982). An operational net shortwave radiation model for glacier basins. *Water Resour. Res.* 18, 220–230. doi: 10.1029/wr018i002p00220

Nascetti, A., Rita, M. D., Ravanelli, R., Amicuzi, M., Esposito, S., and Crespi, M. (2017). Free global dsm assessment on large scale areas exploiting the potentialities of the innovative google earth engine platform. *Int. Arch. Photogramm. Remote Sens. Spat. Inform. Sci.* XLII-1/W1, 627–633. doi: 10.5194/isprs-archives-xlii-1-w1-627-2017

Noh, M.-J., and Howat, I. M. (2017). The surface extraction from TIN based search-space minimization (SETSM) algorithm. *ISPRS J. Photogramm. Remote Sens.* 129, 55–76. doi: 10.1016/j.isprsjprs.2017.04.019

Olson, M. (2019). *Mattols/TopoRad: v1.0 of Topographic Shortwave Radiation Model (Version v1.0)*. Genève: Zenodo. doi: 10.5281/zenodo.2654938

Olson, M., and Rupper, S. (2019). Impacts of topographic shading on direct solar radiation for valley glaciers in complex topography. *Cryosphere* 13, 29–40. doi: 10.5194/tc-13-29-2019

RGI Consortium (2017). *Randolph Glacier Inventory – A Dataset of Global Glacier Outlines: Version 6.0: Technical Report. [Digital Media]*. Colorado, CO: Global Land Ice Measurements from Space. doi: 10.7265/N5-RGI-60

Shea, J. M., Immerzeel, W. W., Wagnon, P., Vincent, C., and Bajracharya, S. (2015). Modelling glacier change in the Everest region, Nepal Himalaya. *Cryosphere* 9, 1105–1128. doi: 10.5194/tc-9-1105-2015

Shean, D. (2017). *High Mountain Asia 8-meter DEM Mosaics Derived from Optical Imagery, Version 1*. Boulder, CO: NASA National Snow and Ice Data Center Distributed Active Archive Center.

Shean, D. E., Alexandrov, O., Moratto, Z. M., Smith, B. E., Joughin, I. R., Porter, C., et al. (2016). An automated, open-source pipeline for mass production of digital elevation models (DEMs) from very-high-resolution commercial stereo satellite imagery. *ISPRS J. Photogramm. Remote Sens.* 116, 101–117. doi: 10.1016/j.isprsjprs.2016.03.012

Sicart, J. E., Hock, R., and Six, D. (2008). Glacier melt, air temperature, and energy balance in different climates: the bolivian tropics, the french alps, and northern sweden. *J. Geophys. Res.* 113, 1–11. doi: 10.1029/2008jd010406

Williams, L. D., Barry, R. G., and Andrews, J. T. (1972). Application of computed global radiation for areas of high relief. *J. Appl. Meteorol.* 11, 526–533. doi: 10.1175/1520-04501972011<0526:aocgrf<2.0.co;2

Wu, S., Wen, J., You, D., Zhang, H., Xiao, Q., and Liu, Q. (2019). Erratum to "algorithms for calculating topographic parameters and their uncertainties in downward surface solar radiation estimation" [aug 17 1149-1153]. *IEEE Geosci. Remote Sens. Lett.* 16, 160–160. doi: 10.1109/lgrs.2018.2868526

Conflict of Interest Statement: The authors declare that the research was conducted in the absence of any commercial or financial relationships that could be construed as a potential conflict of interest.